Wannier function study of the relative stability of zinc-blende and wurtzite structures in the CdX (X = S, Se, Te) series

2008 J. Phys.: Condens. Matter 20 445217

(http://iopscience.iop.org/0953-8984/20/44/445217)

IOP PUBLISHING JOURNAL OF PHYSICS: CONDENSED MATTER

J. Phys.: Condens. Matter **20** (2008) 445217 (8pp) doi:10.1088/0953-8984/20/44/445217

Wannier function study of the relative stability of zinc-blende and wurtzite structures in the CdX (X = S, Se, Te) series

Soumendu Datta[1], **Tanusri Saha-Dasgupta**[1] **and D D Sarma**[2,3]

[1] S N Bose National Center for Basic Sciences, Kolkata 700 098, India
[2] Center for Advanced Materials, Indian Association for the Cultivation of Science, Jadavpur, Kolkata 700 032, India
[3] Solid State and Structural Chemistry Unit, Indian Institute of Science, Bangalore 560 012, India

E-mail: tanusri@bose.res.in

Received 18 July 2008, in final form 17 September 2008
Published 10 October 2008
Online at stacks.iop.org/JPhysCM/20/445217

Abstract

Tetrahedrally coordinated binary II–VI semiconductors are reported to crystallize both in cubic zinc-blende and hexagonal wurtzite structures. The relative stability of these structures and its origin have caught the attention of several researchers in the past. In this work, we revisit this issue for the CdX (X = S, Se, Te) series employing the *N*th-order muffin-tin orbital technique. Our study correctly brings out the trend in this series, providing useful insight in terms of constructed Wannier functions.

(Some figures in this article are in colour only in the electronic version)

1. Introduction

Tetrahedrally coordinated binary semiconductors of $A^N B^{8-N}$ type having a total of eight valence electrons are compounds of great technological importance [1, 2]. They have been widely studied both theoretically and experimentally [3, 4]. An interesting aspect of these compounds is that they can belong to either cubic or hexagonal symmetry types, namely in zinc-blende (ZB) or in wurtzite (WZ) structures. The difference between the two structures is subtle, with both being of tetrahedral coordination, and also the associated total energy difference is small, of the order of a few meV/atom. These particular aspects have made the ZB versus WZ structural stability issue a topic of significant interest that has been discussed in the literature both in terms of model calculations and in terms of first-principles calculations [6–13, 15, 16]. Phillips and Van Vechten [8] first gave a well defined prescription in terms of ionicity for predicting the crystalline phase in binary octet semiconductors of $A^N B^{8-N}$ type, with the help of the dielectric theory. While their theory nicely described the transition from fourfold to sixfold coordination and possibly also to eightfold coordination, it was not able to distinguish clearly between structures having the same coordination. Lawaetz [10] investigated the stability of WZ structure more closely. Taking into account the short-range elastic forces and long-range Coulomb forces, he correlated the ZB versus WZ stability with the deviation of the axial ratio $\frac{c}{a}$ from the ideal value, which was further related to a structure-independent charge parameter. However, the results were not fully satisfactory because of limited knowledge about the long-range Coulomb effects in partially ionic materials. Tomonori [14] achieved some success in systematization of polytypism by relating the energy difference of ZB and WZ phases to a simple empirical formula. Christensen *et al* [15] studied the structural phase stability of 34 elemental and compound semiconductors from first-principles electronic structure calculations which involved mostly transitions from fourfold to sixfold coordination. They studied the chemical trends by calculating the valence charge densities using linearized muffin-tin orbital (LMTO) based localized basis sets. Their calculated ionicities, from tight-binding representation of the LMTO Hamiltonian, gave a better chemical trend than the Phillips values. Recently, the ZB–WZ polytypism in binary octet semiconductors has been studied by Yeh *et al* [16] in terms of quantum mechanically defined atomic orbital radii. They showed a linear scaling between

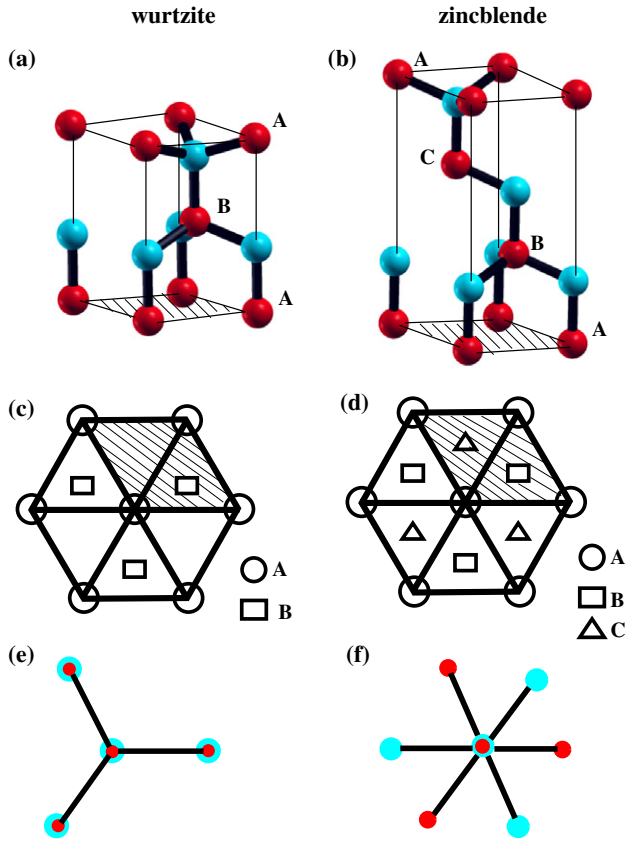

Figure 1. (a) and (b) show the crystal structures in WZ and ZB symmetries. Two different colored atoms denote cations and anions. (c) The WZ structure shows the ABAB $\cdots$ stacking of atoms, while (d) the ZB structure shows the ABCABC $\cdots$ stacking. *Eclipsed* and *staggered* conformations of atoms along the c-axis in the WZ structure and along the [111] body diagonal in the ZB structure are shown in (e) and (f), respectively.

the ZB–WZ energy difference and atomistic orbital radii and successfully predicted the structural trends in most of the octet compounds, except for a few cases. The general understanding that emerged out of all these calculations is that it is the competition between the covalency and the ionicity effects that determines the relative stability of ZB versus WZ structures, with covalency favoring ZB structure and ionicity favoring WZ structure.

Experimentally, the stable crystal phase of CdS at ambient temperature and pressure is hexagonal WZ structure [17]. For CdSe, ZB is the stable low temperature phase and above a critical temperature, it transforms to WZ structure [18]. On the other hand, CdTe always stabilizes in cubic ZB structure [19]. However, there are a few indications of metastable WZ growth for CdTe in some special situations [20]. In the present work, we revisited the issue of relative stability of ZB and WZ in the CdX series, with X = S, Se, Te, using an Nth-order muffin-tin orbital (NMTO) technique [21] within the framework of density functional theory (DFT). In particular, we employed the 'direct generation of Wannier-like orbitals' feature of the NMTO technique for obtaining the microscopic understanding in this context.

Table 1. Structural parameters of ZB and WZ phases for the CdX (X = S, Se, Te) series. Lattice parameters have been taken from [16] for both ZB and WZ phases of CdS, from [22] for ZB CdSe, from [23] for the WZ phase of CdSe, from [19] for ZB CdTe and from [20] for WZ CdTe.

	WZ					ZB
Compounds	a (Å)	$\frac{c}{a}$	u	$\Delta(\frac{c}{a})$	Δu	a (Å)
CdS	4.121	1.621	0.377	−0.012	0.002	5.811
CdSe	4.299	1.631	0.376	−0.002	0.001	6.077
CdTe	4.57	1.637	0.375	0.004	0.000	6.492

2. Crystal structure

The ZB structure consists of two interpenetrating face-centered cubic (FCC) sublattices, one of atoms A, the other of atoms B, displaced from each other along the body diagonal by $\frac{a}{4}$, a being the lattice constant for the ZB structure. On the other hand, an ideal WZ structure consists of two interpenetrating hexagonal close packed (HCP) sublattices, one of atoms A, the other of atoms B, displaced from each other by $\frac{3}{16}c$ along the c-axis. These result in two different stacking sequences: ABCABC $\cdots$ along the [111] direction for ZB and ABAB $\cdots$ along the c-axis for WZ. The ZB structure corresponds to the *staggered* conformation of atomic arrangement along the [111] body diagonal, while the WZ structure corresponds to the *eclipsed* conformation as seen looking down the c-axis. The nearest neighbor (tetrahedral bond) arrangements in the ZB structure and in the ideal WZ structure are identical. The main difference starts to appear in the relative positioning of third-nearest neighbors and beyond. Also the arrangements of the distant atoms along the four different tetrahedral bonds are different for a WZ structure. The structural differences between these two phases are shown in figure 1.

The lower symmetry of the WZ structure allows for a distortion with the c/a ratio deviating from the ideal value of $\sqrt{\frac{8}{3}} = 1.633$. A further kind of distortion, that is possible in the hexagonal structure and forbidden in the cubic, is that the two interpenetrating sublattices are slightly displaced from each other. In order to capture these distortions, it is necessary to define another internal parameter, u, which is the nearest neighbor distance along the c-axis, in units of c. The value u in the ideal WZ structure is $\frac{3}{8} = 0.375$. Deviation of u from its ideal value gives rise to a dipole at the center of each tetrahedron, containing an atom of the opposite kind, the magnitude of which depends upon Δu ($\Delta u = u - 0.375$) and the ionicity of the chemical bonds. This effect also lowers the ionization energy. The structural parameters of CdS, CdSe and CdTe used in the present calculation are listed in table 1.

This shows that the deviation $\Delta(\frac{c}{a})$ ($\Delta(\frac{c}{a}) = \frac{c}{a} - 1.633$) is negative and largest for CdS, while it is positive for CdTe. The deviation from the ideal c/a ratio is tiny for CdSe. The deviation Δu is found to be opposite in sign to that of $\Delta(\frac{c}{a})$. A part of the deviation Δu is expected to arise due to nearest neighbor bond bending or bond stretching caused by $\Delta(\frac{c}{a})$. The limits on this part, as calculated by Keffer and Portis [7] for AlN, are $u = 0.380$, to maintain equal nearest neighbor bond lengths, and $u = 0.372$, to maintain equal four tetrahedral

Table 2. Total energy per formula, energy difference $\Delta E = E(\text{ZB}) - E(\text{WZ})$ and band gaps. The +ve sign of ΔE indicates that WZ is more stable than ZB and vice versa. The numbers within the parentheses in the band gap columns correspond to their experimental values taken from [26].

	Energy (eV/formula)			Band gap (eV)	
Compounds	ZB	WZ	ΔE (meV)	ZB	WZ
CdS	−5.2930	−5.2972	4.2	1.15 (2.55)	1.24 (2.58)
CdSe	−4.7630	−4.7601	−2.9	0.97(1.90)	0.99(1.83)
CdTe	−4.1934	−4.1729	−20.5	0.75(1.60)	0.83(1.60)

angles. However, the measured value of u for AlN is 0.385 [7]. This means that there must be an additional contribution in the distortion of u from the ideal value, which arises from the long-range Coulomb interaction. The NMTO technique based on full self-consistent DFT calculations includes the effect of short-range interaction as well as that of long-range interaction in providing a complete understanding.

3. Total energy calculations

In order to check the relative stability of the ZB and WZ structures of the CdS, CdSe and CdTe, we carried out total energy calculations using the energetically accurate pseudopotential basis set. The calculations have been performed with the projector augmented wave (PAW) method [24] and generalized gradient approximation (GGA) for the exchange–correlation functionals as implemented in the Vienna *ab initio* simulation package (VASP) [25]. The wavefunctions are expanded in the plane wave basis set with a kinetic energy cut-off of 250 eV which gives convergence of total energy sufficient for discussing the relative stability of various phases. The calculations have been carried out with a k-space grid of $11 \times 11 \times 11$. The total energies and the band gaps obtained are listed in table 2. As found, the total energy differences are indeed very tiny; of the order of a few meV. Our calculations correctly show CdS to be stable in the WZ phase and CdTe to be stable in the ZB phase. CdSe, which is considered a borderline case, is found to be stable in the ZB phase in agreement with the published results [16]. The band gaps in WZ and ZB structures, both being direct band gaps for CdS, CdSe and CdTe, are similar for a given compound. As expected, the calculated band gaps are underestimated due to the overbinding problem related to the local density approximation of exchange–correlation functional. It is found that the band gap decreases monotonically in moving from CdS to CdTe in both ZB and WZ symmetries. This monotonic decrease in band gap indicates enhanced metallicity across the CdS → CdSe → CdTe series which points to CdTe being more covalent than CdS.

4. Calculation of the ionicity

As already pointed out, the relative stability of ZB and WZ phases of $A^N B^{8-N}$ semiconductors is dictated by the competition between the covalent bonding and the electrostatic energy given by the difference between the cation and anion energy levels. For homopolar semiconductors like Si, it is only the first term that survives. For a tetrahedrally coordinated semiconductor, it is most natural to think in terms of sp^3 hybrids. Considering the sp^3 hybrid energy as $E_{sp^3} = \frac{E_s + 3E_p}{4}$, the energy level separation between the cation and anion is given by $\Delta E_{sp^3} = E^c_{sp^3} - E^a_{sp^3}$, where c and a denote the cation and anion respectively. The hybridization contribution, on the other hand, is related to the hopping integral, for hopping between the cation and anion sp^3 hybrids. It is given by $h = \frac{1}{4}\langle s^a + p^a_x + p^a_y + p^a_z | H | s^c - p^c_x - p^c_y - p^c_z \rangle$ considering the [111] bond of the ZB structure and $h = \frac{1}{2}\langle s^a + p^a_z | H | s^c - p^c_z \rangle$ considering the [001] bond of the WZ structure where H is the tight-binding Hamiltonian in the sp basis of the cation and anion. The ionicity is then defined as [15]

$$f_i = \frac{(\Delta E_{sp^3})^2}{(\Delta E_{sp^3})^2 + (2h)^2}. \quad (1)$$

In order to extract the energy level separation and the hopping interaction, we employed the NMTO downfolding technique. In this method, a basis set of localized orbitals is constructed from the exact scattering solutions (partial waves and Hankel functions) for a superposition of short-ranged spherically symmetric potential wells, a so called muffin-tin (MT) approximation to the potential. The basis set is constructed from the scattering solutions at a mesh of energies, $\epsilon_0, \epsilon_1, \ldots, \epsilon_N$. At those energies, the set provides the exact solutions, while at other energies, E, the error is proportional to $(E - \epsilon_0)(E - \epsilon_1) \cdots (E - \epsilon_N)$. The basis set of NMTOs is therefore selective in energy. Moreover, each NMTO satisfies a specific boundary condition which gives it a specific orbital character and makes it localized. The NMTO basis set, due to its energy selective character, is flexible and can be chosen as minimal via the downfolding procedure, which integrates out the degrees of freedom that are not of interest. The downfolded NMTO set spans only the selected set of bands with as few basis functions as there are bands. For the isolated set of selected bands the NMTO set spans the Hilbert space of the Wannier functions, that is, the orthonormalized NMTOs are the Wannier functions. The Wannier orbitals are therefore generated directly in this method, which may be contrasted with the techniques where Wannier functions are generated out of the calculated Bloch functions as a post-processing step [27]. The downfolded Hamiltonian in the Wannier basis provides the estimates of on site energies and the hopping integrals.

In order to compute the ionicity parameter defined in equation (1), the NMTO calculations have been carried out

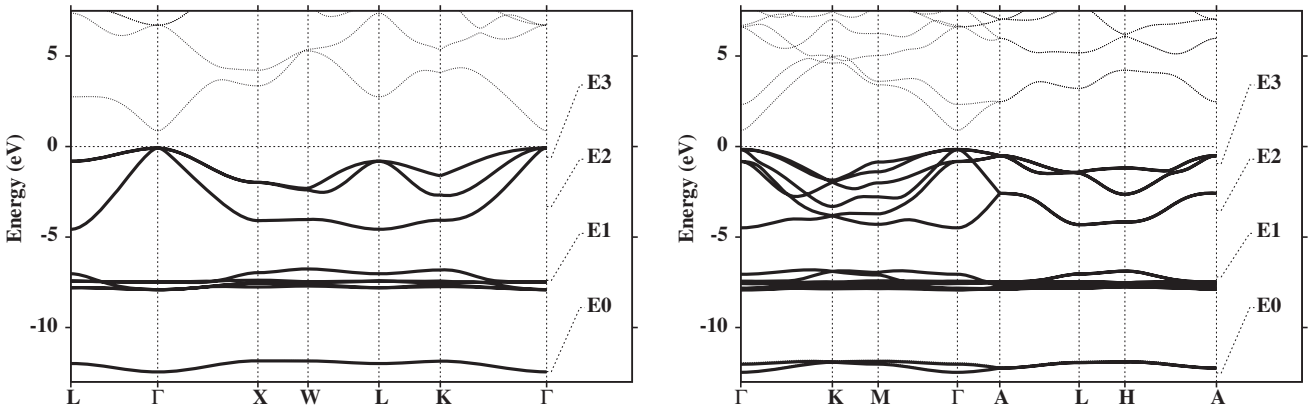

Figure 2. Downfolded bands (thick line) with the basis sets where sp MTOs are on the S atom and d MTOs are on the Cd atom are compared with NMTO for all bands (thin line) both in ZB (left) and WZ (right) structures of CdS. The energy meshes for downfolding have also been shown.

Table 3. Covalent gap ΔE_{sp^3}, hopping term $E_h = -2h$ and ionicity f_i for the CdX series in ZB and WZ structures. f_i (C) means the value of the ionicity calculated by Christensen *et al* from [15], f_i (Ph) that of Phillips taken from [4] and f_i (Pa) that of Pauling taken from [5].

	ΔE_{sp^3} (eV)		$E_h = -2h$ (eV)		f_i				
Compounds	ZB	WZ	ZB	WZ	ZB	WZ	f_i (C)	f_i (Ph)	f_i (Pa)
CdS	7.13	7.17	6.37	6.29	0.556	0.565	0.794	0.685	0.59
CdSe	6.70	6.69	6.16	6.04	0.542	0.551	0.841	0.699	0.58
CdTe	5.36	5.45	5.79	5.74	0.462	0.475	0.739	0.717	0.52

with the Cd (spd) and X (sp) bases. NMTO calculations being not yet implemented in self-consistent form, the self-consistent calculations have been carried out in the LMTO method. The self-consistent MT potential from these LMTO calculations has been used for the constructions of NMTOs, which in the present case is the standard LMTO all-electron CdXEE′ atomic sphere potential for the ZB structure and $Cd_2X_2E_2E'_2$ for the WZ structure. E and E' are two different empty spheres used to fill the space. The calculated estimates of ΔE_{sp^3}, hopping integral h and ionicity parameter f_i for CdX series are listed in table 3. The NMTO approach successfully brings out the right trend within the CdX series both for the ZB and the WZ structures, i.e. CdS has the maximum ionicity and CdTe has the least. For comparison, the results of previous calculations by Christensen *et al* [15] using the tight-binding LMTO approach and those by Phillips [4] using dielectric theory are also listed. As is found, while NMTO could bring out the right trend within the fine differences, the two previous approaches could not capture it properly. For example, both in [15] and in [4] (see table 3) the ionicity of CdSe turned out to be higher than that in CdS. Reference [4] gets CdTe to be of even higher ionicity. We have also compared our results with the Pauling ionicities which are based on empirical heats of formation and are calculated for $A^N B^{8-N}$ compounds from the electronegativity difference via $f_i(Pa) = 1 - \frac{N}{M}\exp(-\frac{|X_A - X_B|^2}{4})$; here $|X_A - X_B|$ is the electronegativity difference between elements A and B, and M is the coordination number. The comparison is presented in table 3.

5. Microscopic understanding in terms of calculated Wannier functions

In order to gain further insights, we went a step further and constructed the truly minimal NMTO sets with the sp orbitals placed exclusively on the anion (X) sites and downfolded all the orbitals at the cation (Cd) sites, except the cation d orbitals. This gives rise to the basis with only 4 sp orbitals out of 8 sp orbitals in the ZB unit cell and 8 sp orbitals out of 16 sp orbitals in the WZ unit cell. The energy points are chosen in such a way as to span only the valence bands. The comparison of the downfolded valence-only bands and the full band structure can be made as good as possible by making the energy mesh finer and finer. The plot shown in figure 2 for CdS with the choice of four energy points already shows the downfolded bands to be indistinguishable from the full band structure on the scale of the plot. Similar agreements are found also for CdSe and CdTe.

Figure 3 shows the plot of the orthonormalized p NMTO ($N = 3$) centered at the anion site and pointing to the neighboring Cd site along the [111] direction for the ZB structure and [001] direction for the WZ structure. As is clearly seen, the gray colored lobe on the left-hand side, which is a mark of the covalency effect, systematically increases in moving from S to Se to Te. Had it been plotted for the case of a homopolar system like Si, which is a perfectly covalent compound, the plot would have been perfectly symmetric, with the gray lobes being symmetric between the left-hand side and the right-hand side. These plots reconfirm the conclusion that the ionicity decreases and the covalency increases across the CdX series.

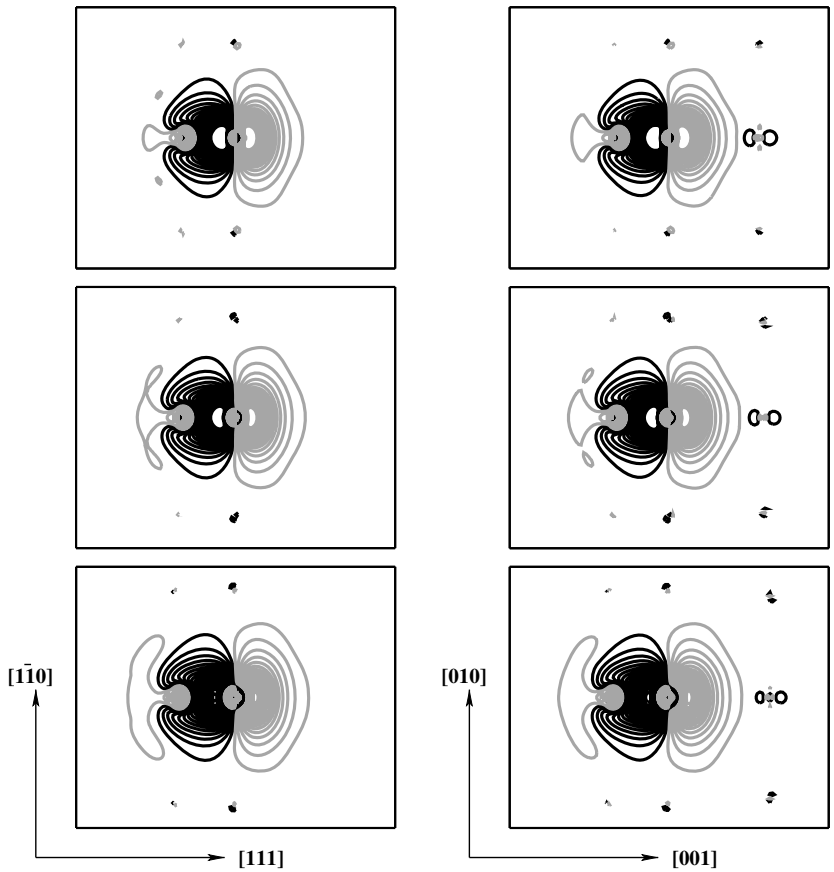

Figure 3. The contour plots show the anion p[111] MTO in ZB structure (left panels) and anion p [001] MTO in WZ structure (right panels) of CdX (X = S, Se, Te). The topmost panels correspond to CdS, the middle panels correspond to CdSe and the bottom panels correspond to CdTe. In each case, 35 contours have been drawn in the range −0.15 to 0.15 electrons Bohr^{-3}. From top to bottom, the ionicity decreases and the covalency increases.

Table 4. Covalent gap ΔE_{sp^3}, hopping term $E_h = -2h$ and ionicity f_i for the model CdTe in the WZ structure, with $\Delta(\frac{c}{a})$ and u as given in the first column.

CdTe	ΔE_{sp^3} (eV)	$E_h = -2h$ (eV)	f_i
$\Delta(\frac{c}{a}) = -0.100$ and $u = 0.4044$	5.49	5.33	0.515
$\Delta(\frac{c}{a}) = -0.050$ and $u = 0.3903$	5.48	5.57	0.491
$\Delta(\frac{c}{a}) = +0.004$ and $u = 0.375$	5.45	5.73	0.475
$\Delta(\frac{c}{a}) = +0.100$ and $u = 0.3432$	5.45	6.13	0.441

Figure 4 shows the plots of directed p NMTO, as in figure 3, but for four different tetrahedral bond directions of WZ and ZB structures for CdS. While the four bond-centered p NMTOs look identical for ZB structure, the bond-centered p NMTO directed along the [001] direction of the WZ structure looks different from the rest of the three. The difference primarily comes from the tail sited at the Cd position at $c(1-u)$ measured from the central anion position at X, (0, 0, 0), along the [001] axis (see figure 5). There is no equivalent neighboring atom along the other three directions.

In order to understand this effect, we have carried out model calculations where the $\Delta(\frac{c}{a})$ ratios have been made -0.1, -0.05 and 0.1. The corresponding u parameter in each case has been obtained by total energy minimization, fixing the lattice parameters. The deviation in u, Δu, is found to roughly obey the relationship with $\Delta(\frac{c}{a})$ as $\Delta u = -(\frac{3}{128})^{\frac{1}{2}}\xi\Delta(\frac{c}{a})$ where ξ, the bond-bending parameter, is 2.0, given by Lawaetz [10]. We computed the ionicity parameter f_i for each of the model systems by the NMTO downfolding technique. In table 4 we list the ionicity parameter for the model WZ systems, together with the actual CdTe case. Evidently, the negative deviation from the ideal $(\frac{c}{a})$ ratio makes the compound more ionic, as pointed out previously. Changing the $\Delta(\frac{c}{a})$ ratio from negative to positive, passing through the ideal $\Delta(\frac{c}{a})$ ratio, the ionicity decreases and covalency increases. This is in agreement with the structural parameters of CdS, CdSe and CdTe. CdS, being the most ionic among the three, shows the largest negative deviation in $(\frac{c}{a})$. The $(\frac{c}{a})$ ratio for CdSe is close to ideal, while deviation in the $(\frac{c}{a})$ ratio for CdTe becomes positive.

In figure 6, we show the downfolded p NMTO for the model WZ systems together with actual WZ CdTe system

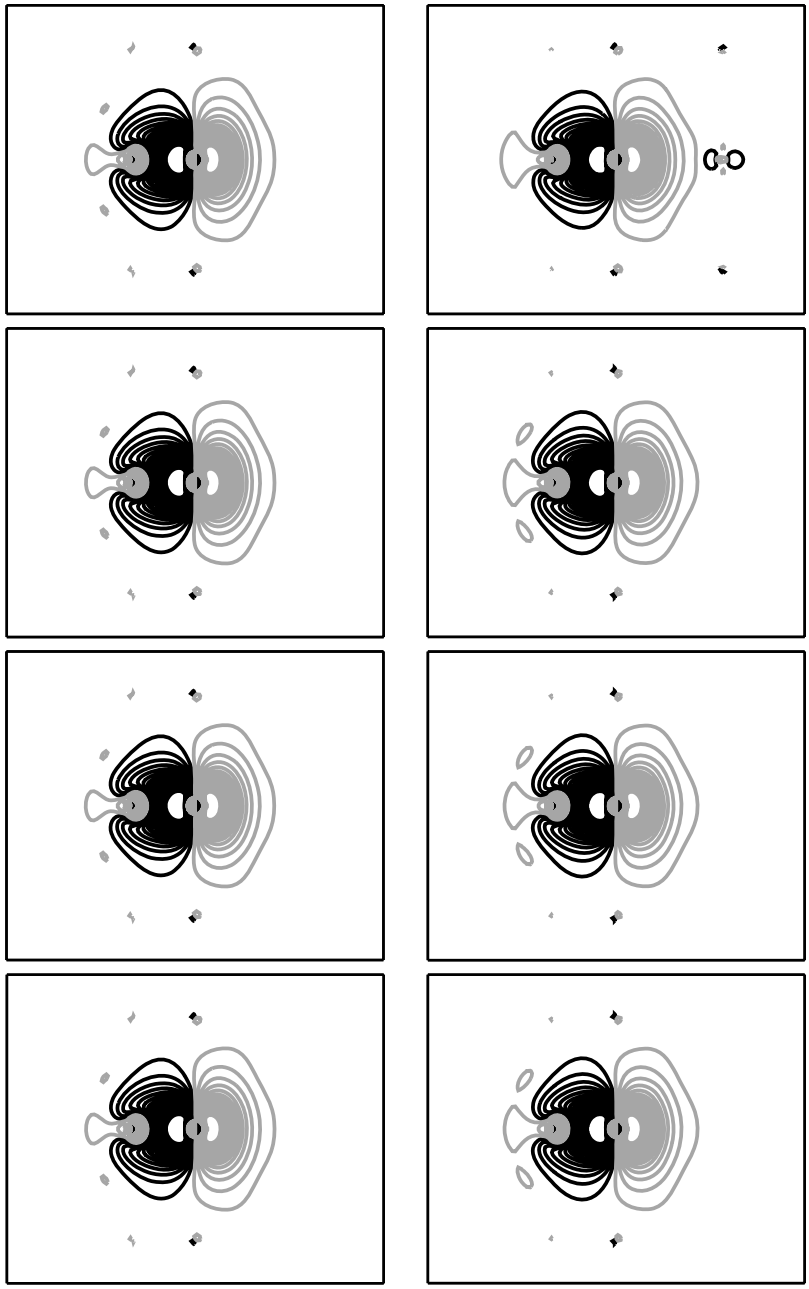

Figure 4. The contour plots show the p MTO of S along the four nearest neighbor tetrahedral directions in ZB structure (left panels; from top to bottom they are p [111], p[1$\bar{1}\bar{1}$], p[$\bar{1}$1$\bar{1}$], p[$\bar{1}\bar{1}$1]) and in WZ structure (right panels; from top to bottom they are p [001], p[1, 0, $\frac{u}{\sqrt{3}}\frac{c}{a}$], p[$\frac{1}{2}$, $-\frac{\sqrt{3}}{2}$, $-\frac{2}{\sqrt{3}}u\frac{c}{a}$], p[$\frac{1}{2}$, $\frac{\sqrt{3}}{2}$, $-\frac{2}{\sqrt{3}}u\frac{c}{a}$]) of CdS. The contours chosen are the same as in figure 3.

along the [001] direction and one of the three other directions, namely [1, 0, $\frac{u}{\sqrt{3}}\frac{c}{a}$]. As is evident, changing $\Delta(\frac{c}{a})$ from negative to positive makes the two p NMTOs directed along the vertical [001] bond and one of the other directions look alike, diminishing the tail effect sited at the Cd [0, 0, $c(1-u)$] site. This is driven by the covalency effect which favors an isotropic arrangement. However, it cannot be completely achieved within a hexagonal symmetry; a compound with nearly ideal $(\frac{c}{a})$ or positive $\Delta(\frac{c}{a})$ ratio therefore 'prefers' to stabilize in ZB symmetry, satisfying the isotropic distribution completely.

In order to have quantitative estimates of ionicity based on truly minimal Wannier functions, we have also computed the shift of the center of gravity of the Wannier function from the bond center, introduced by Abu-Farsakh *et al* [28] as $\beta = r/d$; here r is the distance between the center of gravity of the Wannier function and the position of the cation of the associated bond, and d is the bond length. Table 5 contains our calculated values of bond ionicities β for the CdX series in both ZB and WZ structures. The calculated bond ionicity β gradually decreases and shows the right trend in the CdX series, as we obtained using equation (1).

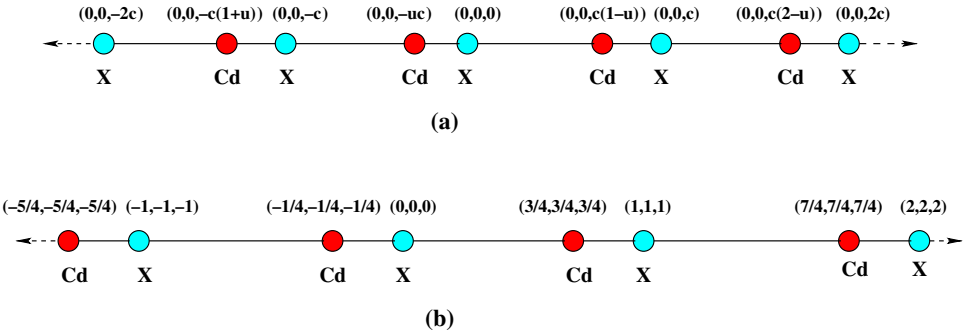

Figure 5. (a) Positions of atoms along the [001] direction of wurtzite structure; (b) positions of atoms in units of the lattice constant along the [111] direction of zinc-blende structure.

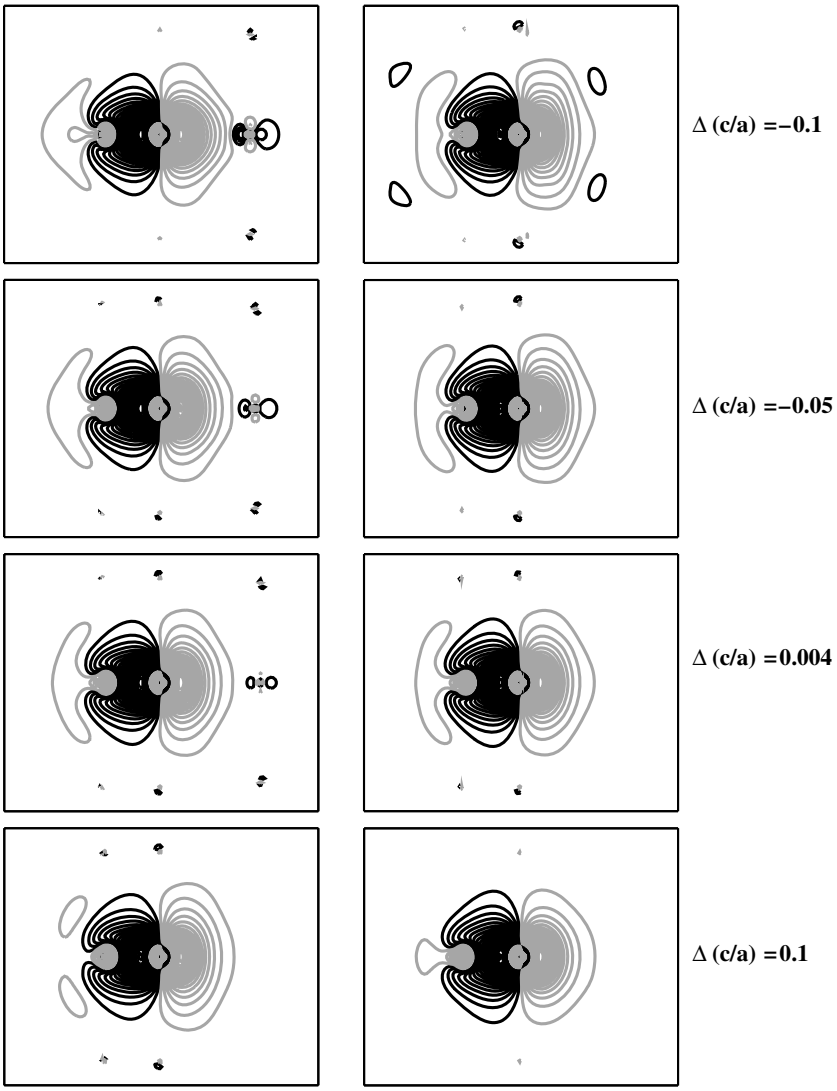

Figure 6. The above contour plots show the p MTO of Te in the WZ structure of the model CdTe. The left panels correspond to p[001] and the right panels correspond to p[1, 0, $\frac{u}{\sqrt{3}}\frac{c}{a}$]. From top to bottom, ionicity decreases and covalency increases, and the distribution becomes more isotropic. The contours chosen are the same as in figure 3.

6. Summary

Using the NMTO downfolding technique we have revisited the problem of ZB versus WZ symmetry in the case of $A^N B^{8-N}$ semiconductors. In particular, we have considered the CdX series with X = S, Se, Te. Our ionicity factors computed using accurate NMTO downfolding successfully bring out the right trend within the CdX series—CdS, being most ionic, stabilizes

Table 5. The bond ionicity, β, for the CdX series in both ZB and WZ structures.

Compounds	ZB	WZ
CdS	0.745	0.745
CdSe	0.739	0.743
CdTe	0.708	0.714

in WZ symmetry while CdSe and CdTe, being more covalent, stabilizes in ZB symmetry. Our NMTO constructed Wannier functions corresponding to only valence bands highlight this fact. Bond ionicity measurement using the displacement of the center of the Wannier function from the bond center also shows the right trend. The tendency towards ZB stability is governed by the covalency which favors an isotropic nature of the tetrahedral bonds.

Acknowledgments

SD thanks the Council of Scientific and Industrial Research (Government of India) for financial support. TSD and DDS acknowledge the Department of Science and Technology (Government of India) for support through Swarnajayanti and J C Bose fellowships, respectively.

References

[1] Jain M (ed) 1993 *II–VI Semiconductor Compounds* (Singapore: World Scientific)
[2] Birkmire R W and Eser E 1997 *Annu. Rev. Mater. Sci.* **27** 625
[3] Harrison W A 1980 *Electronic Structure and the Properties of Solids* (San Francisco, CA: Freeman)
[4] Phillips J C 1973 *Bonds and Bands in Semiconductors* (New York: Academic)
[5] Adachi S 2005 *Properties of Group-IV, III–V and II–VI Semiconductors* (New York: Wiley)
[6] Jeffrey G A, Parry G S and Mozzi R L 1956 *J. Chem. Phys.* **25** 1024
[7] Keffer F and Portis A M 1957 *J. Chem. Phys.* **27** 675
[8] Phillips J C and Van Vechten J A 1969 *Phys. Rev. Lett.* **22** 705
[9] Phillips J C 1970 *Rev. Mod. Phys.* **42** 317
Van Vechten J A 1969 *Phys. Rev.* **187** 1007
[10] Lawaetz P 1972 *Phys. Rev.* B **5** 4039
[11] John J S and Bloch A N 1974 *Phys. Rev. Lett.* **33** 1095
[12] Zunger A and Cohen M L 1978 *Phys. Rev. Lett.* **41** 53
[13] Zunger A 1980 *Phys. Rev. Lett.* **44** 582
Zunger A 1980 *Phys. Rev.* B **22** 5839
[14] Ito T 1998 *Japan. J. Appl. Phys.* **37** L1217–20
[15] Christensen N E, Satpathy S and Pawlowska Z 1987 *Phys. Rev.* B **36** 1032
[16] Yeh C-Y, Lu Z W, Froyen S and Zunger A 1992 *Phys. Rev.* B **45** 12130
Yeh C-Y, Lu Z W, Froyen S and Zunger A 1992 *Phys. Rev.* B **46** 10086
[17] Rittner E S and Schulman J H 1943 *J. Phys. Chem.* **47** 537
[18] Fedorov V A, Ganshin V A and Korkishko Yu N 1991 *Phys. Status Solidi* **126** K5
[19] Rabadanov M Kh, Verin I A, Ivanov Yu M and Simonov V I 2001 *Kristallografiya* **46** 703
[20] Semiletov S A 1955 *Trudy Inst. Kristallogr. Acad. Nauk SSSR* **11** 121–3 from ICSD
[21] Andersen O K and Saha-Dasgupta T 2000 *Phys. Rev.* B **62** R16219 and references therein
[22] Lao P D, Guo Y, Siu G G and Shen S C 1993 *Phys. Rev.* B **48** 11701
[23] Stevenson A W and Barnea Z 1984 *Acta Crystallogr.* B **40** 530
[24] Blöchl P E 1994 *Phys. Rev.* B **50** 17953
[25] Kresse G and Hafner J 1993 *Phys. Rev.* B **47** RC558
Kresse G and Hafner J 1993 *Phys. Rev.* B **48** 13115
Kresse G and Hafner J 1994 *Phys. Rev.* B **49** 14251
[26] Hellwege K-H and Madelung O (ed) 1982 Numerical data and functional relationships *Science and Technology* (*Landolt–Börnstein, New Series* Group III, vols 17a and 22a) (New York: Springer)
[27] Marzari N and Vanderbilt D 1997 *Phys. Rev.* B **56** 12847
[28] Abu-Farsakh H and Qteish A 2007 *Phys. Rev.* B **75** 085201